Friction Stir Welding of Steel for Pipeline Fabrication

Grégory Toguyeni; Christian Pfeiffer, Dr. Ozan Caliskanoglu, Lucas Oppeneiger > Subsea 7 France; Stirtec GmbH

Abstract

Friction stir welding procedure development was initiated on steel grades S460 G2+M and S690QL1 in plate wall thicknesses of 10 and 15mm. To tackle the challenges of the high mechanical loads on the tool as well as its premature wear, a combination of preheating and optimized weld backing set-up was implemented. The inductive preheating allowed a 28% reduction in welding torque and a significant reduction of the tool wear, particularly during the critical initial plunge of the tool within the base material. A comparison of Mo-based and W-based tool was performed, allowing identifying the W-based tool as having a better combination of high temperature strength and wear resistance. Different backing arrangements and materials were investigated. Ceramic backing inlays were used to reduce the heat loss at the root area and maintain an acceptable stirring of this zone to achieve full penetration welds. The welds quality was assessed via metallurgical examination, bend tests and confirmed the possibility to perform sound full-penetration, one-sided welds. The contribution of the preheating to the process as well as the quality and mechanical properties of the welds will be presented here. Finally, the transfer of the process parameters to pipe welding were started and will be discussed here.

1. INTRODUCTION

The welding processes currently used for the fabrication of steel pipelines have essentially remained the same for the last 35 years. They all consist in multi-pass arc welding with various degrees of mechanisation and electrical waveform control. The strengths and weaknesses of such processes are now well understood and accounted for by the welding engineers. Among the weaknesses of multi-pass arc welding is the high propensity for weld defects, either between the weld and the adjacent substrate or between weld passes. The individual weld beads microstructure being closer to that of a casting, the achievement of the required mechanical properties depends strongly on the selection of the appropriate welding filler metal and the welding sequence. The weld geometry, at the cap and root, can also be detrimental to the fatigue resistance of the welded assembly. To further advance automation but also improve welds quality and mechanical properties, Friction Stir Welding (FSW) has been assessed as a potential disruptive technology. It also has the potential to allow high strength steel welding for deep-water applications. It is a solid-state one-shot process using a rotating tool to generate frictional heat at the interface between the parts to be welded. The substrate is softened and consolidated into a weld while contained between the tool and a backing support. The process is autogenous, and the weld mechanical properties are directly linked to the composition and metallurgy of the base material. Being a one-shot process, it allows a better control and a reduction of weld defects. It has also been suggested that the weld geometry offers better fatigue performances than arc welds.1

he economic viability of FSW depends on the context of application. The development costs as well as the machine and tool costs should be taken into consideration. For the welding of offshore pipelines, one of the key factors is productivity. With the welding operations performed on the lay vessel or on the quayside, any improvement in the number of weld performed per working shift can represent significant cost savings in terms of vessel or spoolbase working time.2 Considering typical Gas Metal Arc Welding (GMAW) cycle times from an offshore pipeline fabrication contractor's track records, with the welding operations performed in one work station (J-lay installation method), the FSW offers a welding cycle time advantage when the tool travel speed is above 2 mm/s on a 12" OD x 15.9mm thick pipe. At a travel speed of 4 mm/s the FSW is 30.3% faster than GMAW; this can represent a cost saving per weld in excess of 3000€. Additionally, better fatigue performances and the option to weld higher strength steels could allow more flexibility on pipeline and riser designs, thus generating additional cost savings to projects.

Already strong of a significant industrial application track record for aluminium welding, the process adaptation to steel presents several key challenges. Three of these are:

1) High mechanical loads on the tool
2) High tool wear and
3) Achieving consistent full penetration on one-sided welds performed on wall thicknesses representative of the offshore pipeline industry.

2 SCOPE AND OBJECTIVES

A combination of local pre-heating centered on the joint and back-wall insulation was implemented. The preheating parameters development was made after a detailed investigation of the through-thickness temperature distribution. The objective was to find the correct set of preheating parameters to sufficiently soften the base material through thickness to reduce the welding loads and tool wear while not excessively tempering the steel mechanical properties outside of the weld zone, in the heat affected zone (HAZ). The targeted maximum pre-heating temperature at 25mm away from the weld centerline was 600°C. A backing arrangement was necessary to counteract the welding down-force and retain some heat around the weld root. It has been established that good stirring of the root area is correlated to sufficient base material temperature in this zone, especially on thicker one-sided welds. Full penetration welds are in effect a requirement for pipeline girth welding.

3 EXPERIMENTAL PROCEDURE

Linear bead-on-plate (BOP) and butt welds of 200 - 250mm in length were produced to investigate the lifetimes of molybdenum- and tungsten-based FSW tools by producing fully consolidated, full penetration welds. The experimental setup is summarized in Table 1. Steel plates of grade S460 G2+M and S690 QL1 with a thickness of 10mm and 15mm have been investigated for the study. The respective chemical compositions are given in Table 2.

Table 1: Experimental setup for FSW-study on steels

FSW-tool	Welded steels	Welding speed [mm/min]	Welding depth [mm]
Mo-based	S460 G2+M	80 - 180	10
W-based	S460 G2+M, S690 QL1	120 - 360	10, 15

Table 1: Experimental setup for FSW-study on steels

Table 2: Chemical composition of the investigated steels (wt. - %)

Steel grade	C	Si	Mn	P	Cr	Ni	Cu	Nb	Ti
S460 G2+M	0,03	0,34	1,64	0,009	0,173	0,18	0,16	0,04	0,013
S690 QL1	0,15	0,29	1,45	0,012	0,329	0,03	0,02	0,02	0,013

Table 2: Chemical composition of the investigated steels (wt. - %)

The experiments on plate have been performed on a custom-built Stirtec‡ FSW-machine with a maximum downforce of 100 kN, a maximum spindle torque of 330 Nm and a maximum spindle speed of 3000 rpm. It is equipped with a cooling head and a 50kW inductive preheating system for a localized and controlled heat input in front of the FSW tool to preheat steel plates with a thickness up to 25 mm.

The used tools consist of a shoulder with a diameter of 25mm for 10mm and 32mm for 15mm thick plates and an unthreaded and tapered probe. Both tool materials can be easily redressed to their original design once excessive tool wear has been observed.

For a specific plate thickness and welding speed, the optimum temperature evolution during the preheating process on the top and bottom plate sides was determined since it has proved to markedly decrease the welding loads and tool wear during welding, respectively.3,4 This includes the stationary heating for the tool plunging phase and an instationary heating for the tool travel phase. Figure 1 shows the thermocouples setup used for both conditions.

Furthermore, different backing inlay materials were used for both mechanical support and thermal insulation to facilitate sound weld quality. To test these backing materials, a baseplate with exchangeable backing and insulating inlays was designed as shown in Figure 2. Different types of insulating and backing materials were tested including steels, ceramics and tungsten carbides.

To qualify the weld, metallographic analyses were carried out on transversally sectioned weldments, which were polished and etched in a 3% Nital solution. Moreover, the weld quality was evaluated by hardness tests, tensile tests, as well as face and root bend tests. The tool wear was evaluated by optical assessment and by X-ray fluorescence (XRF)-analyses on the weldments.

Before transferring the results from the plate to pipe and to weld higher grade materials at higher welding depths, an upgrade of the machine was performed. The machine was additionally mechanically reinforced, and a more powerful spindle was installed to enable a maximum torque of 600Nm and a radial force up to 40kN.

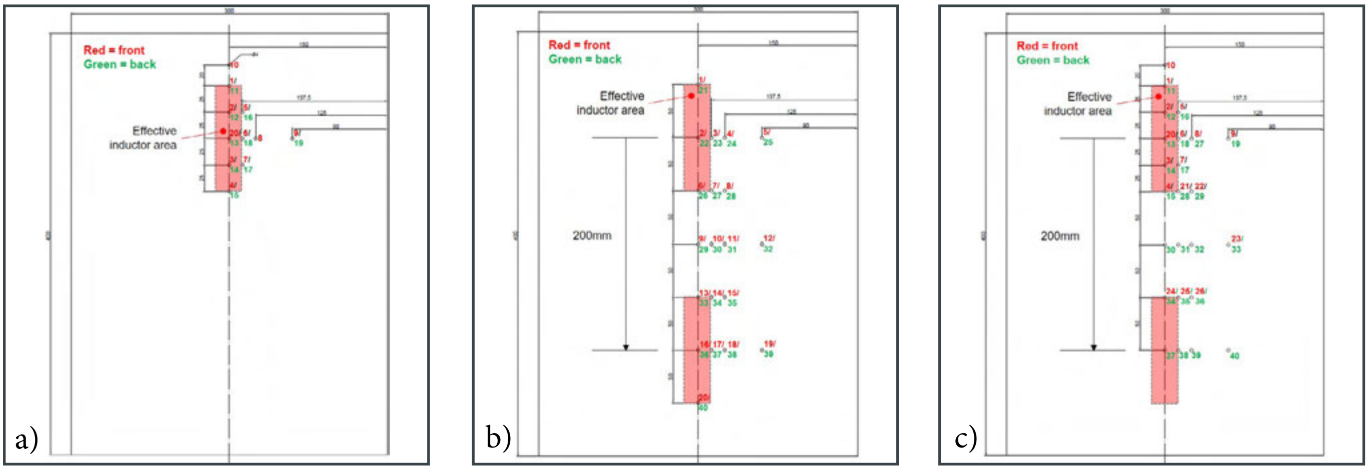

Figure 1: Thermocouple setup for a) 10 and 25mm thick stationary, b) 10mm and c) 25 mm thick instationary preheating tests

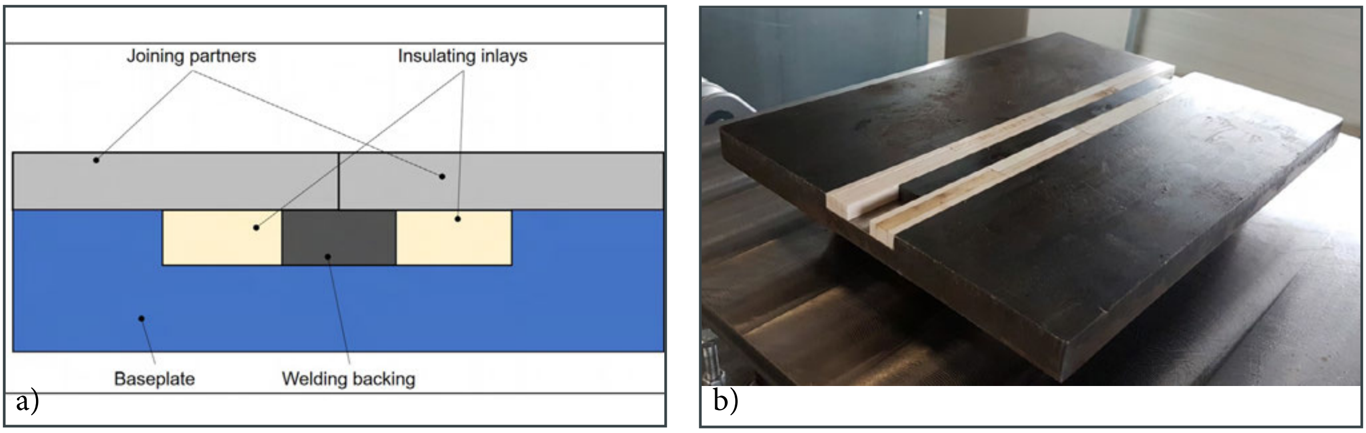

Figure 2: a) Schematic representation of the used backing setup, b) setup ready for use

To be able to weld pipes, an additional pipe rotating system was designed and manufactured as shown on Figure 3. The weldable pipe diameter ranges from 8-12 inch (NPS). The system is designed to fit two 600mm coupons for butt welding or 1400mm long single pipes for bead-on- pipe configuration. During the welding process the pipes are aligned, clamped and supported in the welding area by an internal backing system which fits the standard pipe tolerances. Exchangeable backing and insulating inlays can be placed in the backing system (comparable to the setup for the plate welds to simplify the parameters transfer). A new inductor was produced to fit the curved shape of the pipe and it can automatically be retracted from the surface.

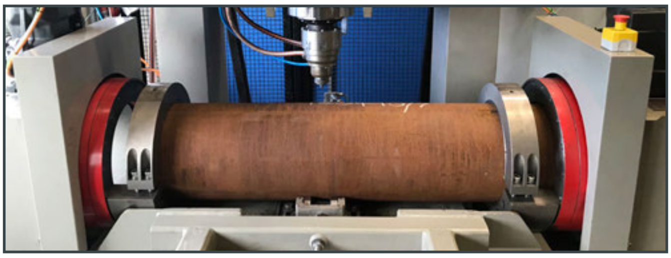

Figure 3: Weld set up for pipe welding

4 RESULTS

4.1 PREHEATING TESTS

The aim of the preheating tests was to determine the required parameters for through-thickness heating of the base material without both overheating the face side of the plate and impairing the mechanical properties next to the inductor and FSW tool shoulder region. The preheating parameters were chosen in order not to exceed 600°C in the future HAZ. The future stir zone of the weld was allowed to reach higher temperatures. This activity was part of the calibration process of the preheating system. Figure 4 shows the temperature curves during stationary preheating of a 10mm thick S460 G2+M plate. The maximum temperature difference between top and root side was 120-140°C along the front and back inductor edge and only 40°C in the center region. Compared to the 10 mm thick steel, the temperature gradient on the stationary 25mm S460 G2+M plate was significantly higher. The difference between top and root side was around 400°C at the inductor boundaries and 225 °C in the middle (Figure 5). A higher heat input to achieve higher temperatures on the root side caused an overheating of the base material next to the inductor.

a)

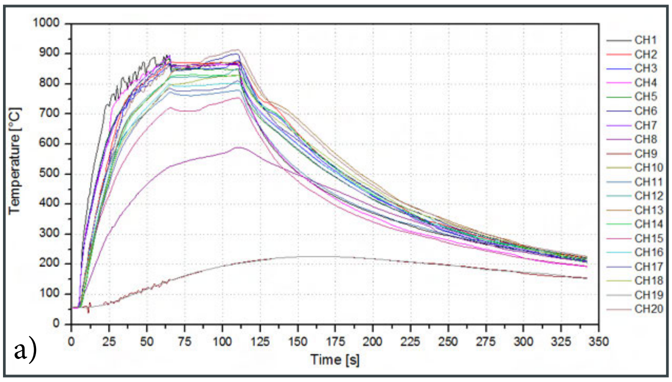

b)

Front		Back		ΔT
TC	[°C]	TC	[°C]	[°C]
1	900	11	780	120
2	875	12	850	25
5	885	16	800	85
20	915	13	875	40
6	900	18	830	70
9	225	19	225	0
3	880	14	830	50
7	895	17	810	85
4	895	15	755	140
8	590			
10	Not used			

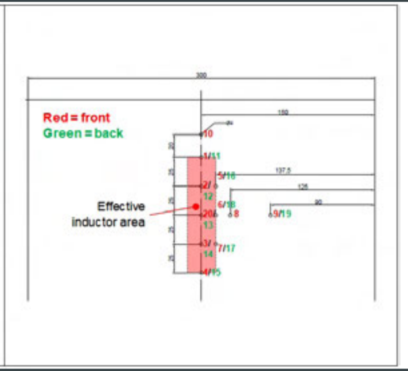

Figure 4: a) Temperature curves and b) peak temperatures of the thermocouples for stationary preheating of a 10 mm thick S460 G2+M plate

a)

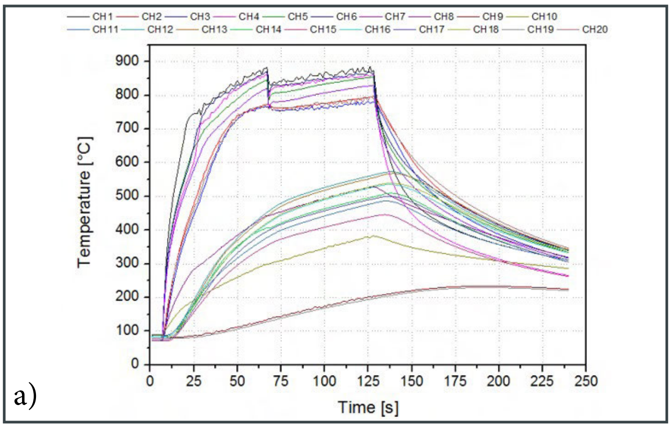

b)

Front		Back		ΔT
TC	[°C]	TC	[°C]	[°C]
1	885	11	485	400
2	800	12	575	225
5	855	16	535	320
20	795	13	570	225
6	870	18	540	330
9	235	19	230	5
3	780	14	510	270
7	830	17	500	330
4	865	15	445	420
8	530			
10	385			

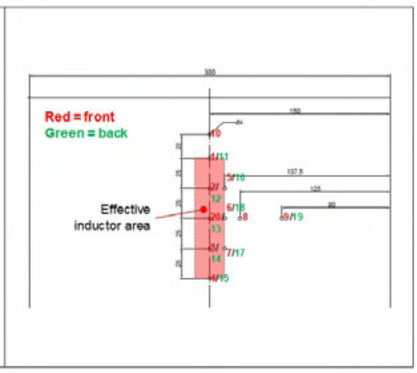

Figure 5: a) Temperature curves and b) peak temperatures of the thermocouples for stationary preheating of a 25 mm thick S460 G2+M plate

To determine the preheating parameters during welding, instationary preheating tests have been performed. For the 10mm tests, the temperature evolution during travelling showed a slight difference between top and root area (see Figure 6). In contrast, the root temperature on the 25mm plates (shown in Figure 7) was significantly lower compared to the 10mm plate tests.

4.2 INFLUENCE OF PREHEATING ON THE TOOL WEAR

To determine the influence of a preheated base material, extensive series of weld tests with the Mo-based tool were carried out. Tests showed that most of the tool wear occurs during the plunging process. To minimize this effect, the steel plate was preheated in the plunging area before the rotating tool plunged into the base material.

To classify the wear, the length of the probe and the shoulder of the tool was measured after each plunge test. Especially the probe shows a considerable wear caused by the plunging process. Figure 8 shows a new and a used tool where this wear behavior is clearly visible. In Figure 9, the wear after 10 plunges, which means a contact time of the tool to the base material of around 250 second (~ 25 seconds per plunge) and 10 weld seams (each 250mm long), which means a contact time between tool and base material of 1500 s (~ 25 seconds per plunge and 125 s per weld seam) is shown. Comparing these results shows that 40 % of the length reduction of the probe happens during the plunging process which only represents 17 % of the process time (contact between tool and base material). Preheating reduced this wear significantly. Figure 9a shows the influence of preheating on the tool wear.

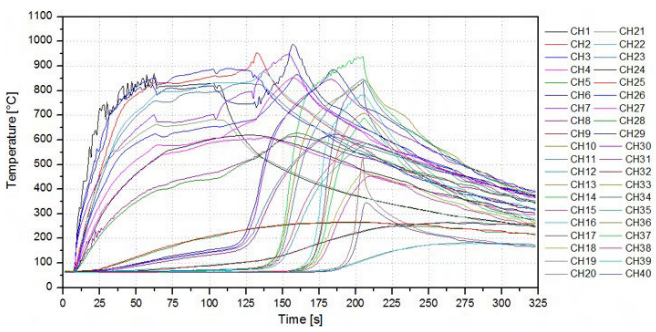

a)

Front		Back		ΔT [°C]
TC	[°C]	TC	[°C]	
1	870	21	685	185
2	955	22	875	80
3	900	23	830	70
4	610	24	620	-10
5	265	25	265	0
6	990	26	865	125
7	950	27	850	100
8	615	28	630	-15
9	failed	29	885	-
10	930	30	845	85
11	615	31	620	-5
12	265	32	265	0
13	failed	33	845	-
14	940	34	845	95
15	590	35	585	5
16	785	36	710	75
17	840	37	685	255
18	470	38	450	20
19	185	39	180	5
20	525	40	345	180

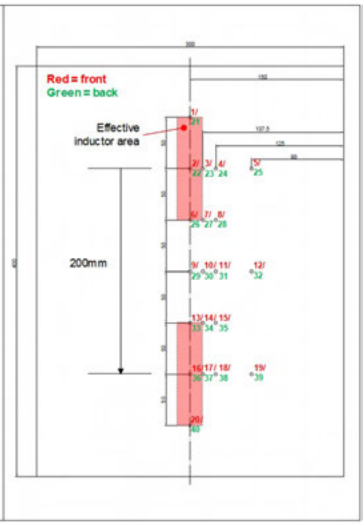

b)

Figure 6: a) Temperature curves and b) peak temperatures of the thermocouples for instationary preheating (travel speed of 120mm/min) of a 10 mm thick S460 G2+M plate

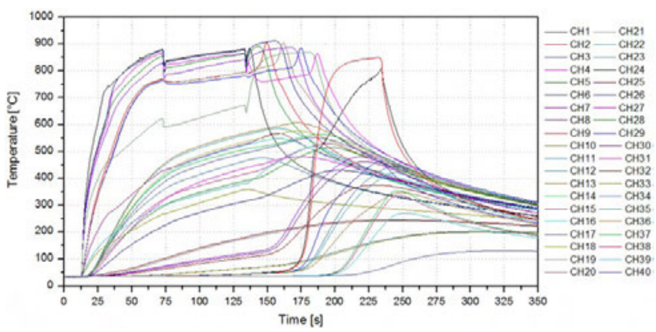

a)

Front		Back		ΔT [°C]
TC	[°C]	TC	[°C]	
1	885	11	475	410
2	905	12	585	320
5	890	16	550	340
20	905	13	605	300
6	915	18	575	340
9	245	19	240	5
3	885	14	565	320
7	890	17	550	340
4	870	15	530	340
8	570	27	480	90
10	360			
21	870	28	515	355
22	520	29	430	90
23	200	33	200	0
24	810	34	445	365
25	850	35	420	430
26	465	36	345	120
		30	480	
		31	460	
		32	375	
		37	350	
		38	335	
		39	270	
		40	130	

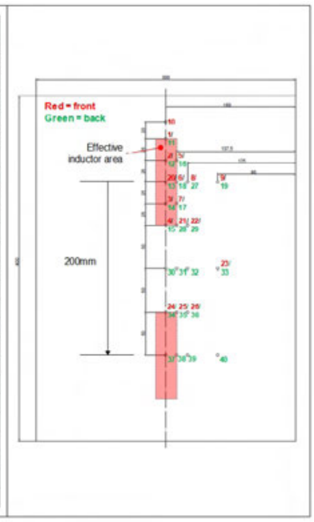

b)

Figure 7: a) Temperature curves and b) peak temperatures of the thermocouples for instationary preheating (travel speed of 120mm/min) of a 25 mm thick S460 G2+M plate

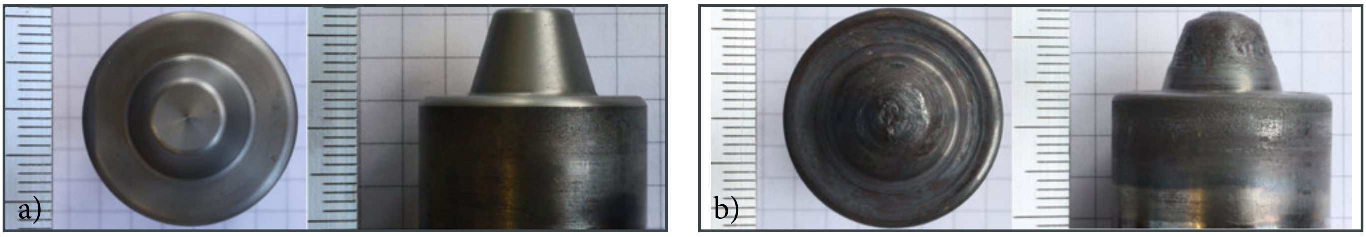

Figure 8: a) Unused Mo-based tool, b) Mo-based tool after 10 plunges without preheating

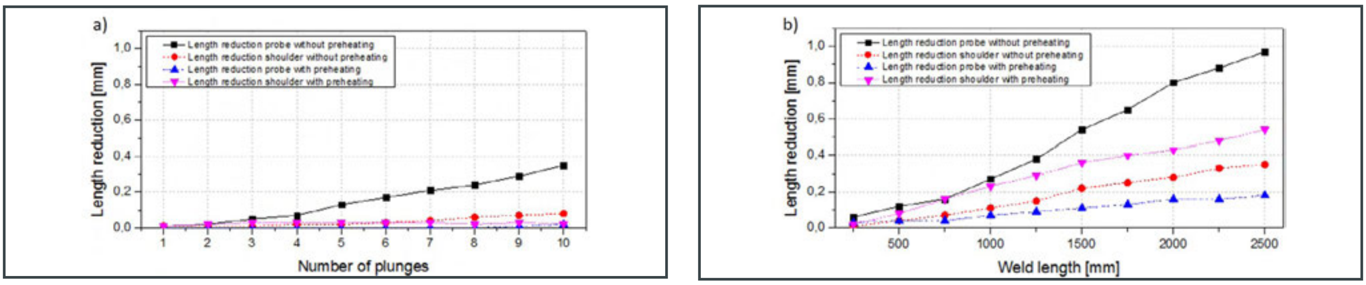

Figure 9: Length reduction during wear tests performed with a featureless Mo-based tool a) length reduction during plunging, b) length reduction during plunging and welding

During welding, the heat input of the preheating system was reduced to an amount that did not overheat the base material but still provides the beneficial effect on the tool wear. The wear was measured every 250mm for both set-ups. The results (shown in Figure 9b) showed a reduction in wear on the probe and a slight increase on the shoulder when preheating was applied. These tests were performed with the Mo-based tool. The W-based tool showed better wear behavior later during welding compared to the Mo-based tool.

4.3 INFLUENCE OF PREHEATING ON THE MACHINE LOADS

Preheating of the base material affects the welding process parameter and therefore the load on the welding machine. For thick section welding, this effect can be beneficial. To display the reduction potential, Table 3 shows two 10mm S460 G2+M steel grade weld tests performed with a Mo-based tool. One was performed with and the other one without preheating.

Table 3: Load reduction caused by preheating

	Without preheating	With preheating	Reduction [%]
Spindle torque [Nm]	310	230	28
Welding force [kN]	44	38	13,5

Table 3: Load reduction caused by preheating

4.4 S460 G2+M WELDING DEVELOPMENT

Starting with the Mo-based tool and bead-on-plate weld seams, a process development on 10mm thick S460 G2+M plates was performed. The process was then transferred to weld seams in butt configuration on two 150mm wide plates with square milled sides.

Figure 10 shows a cross section of one of the test welds. On the advancing side (AS) of the weld seam 5-7 mm under the cap side a dark region can be found. EDX analysis confirmed the assumption that this is a concentration of wear particles from the tool. Figure 11 shows the higher molybdenum content in the examined area.

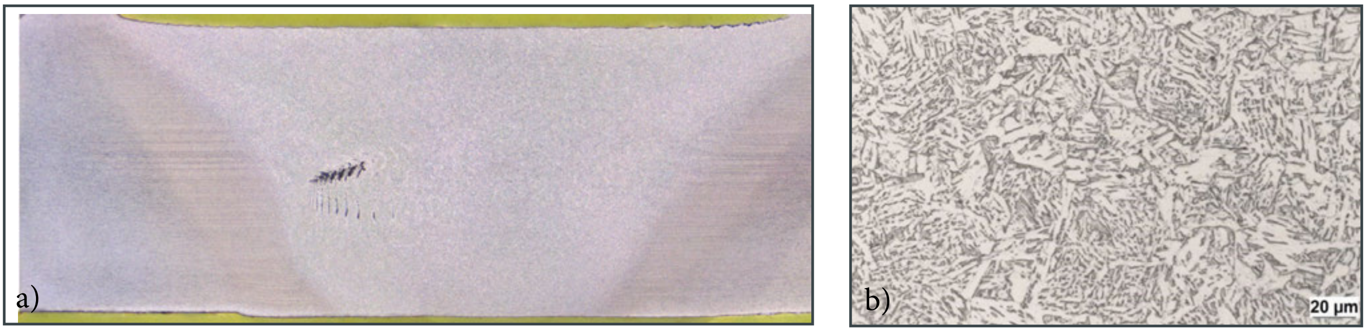

Figure 10: a) Cross section and b) microstructure of the weld zone of a 10mm S460 G2+M weld seam performed with a Mo-based tool.

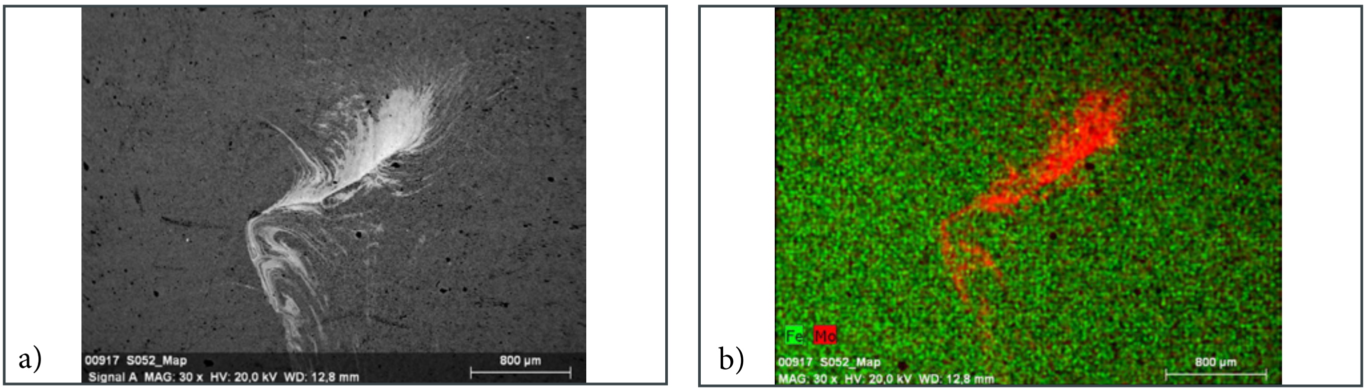

Figure 11: SEM-EDX analysis around the inhomogeneous zone on the AS of the FSW weld a) SEM picture and b) Fe-Mo mapping

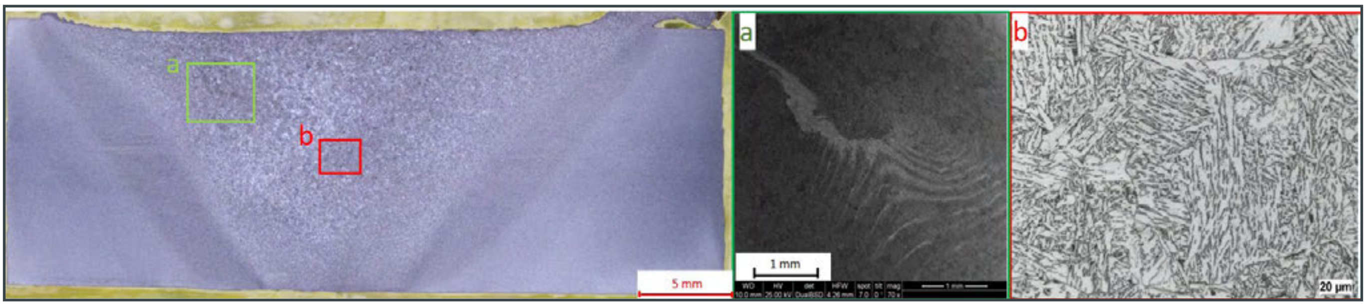

Figure 12: Characterization of the tool wear in a 15mm thick S460 G2+M weld seam performed with a W-based alloy tool.

Table 4: wt. % of tool wear elements on weld seams with Mo and W-based tools

Element	Base metal S460 G2+M	XRF-analysis [wt.%], advancing side: Welded with Mo-based tool	XRF-analysis [wt.%], advancing side: Welded with W-based tool
Mo	0,01	0,29	0,013
W	0,002	0,005	0,04

Table 4: wt. % of tool wear elements on weld seams with Mo and W-based tools

In the next step, the welding depth was increased to 15mm. For the increased welding thickness, the Mo-based tool was not capable to perform sound weld seams. The wear on the tool was too high and with the increased tool load associated to the higher welding depth the probe started to deform. Therefore, the tool material was changed to a tungsten-based alloy. The new tool material showed less wear and a higher rigidity.

This change led to an adaptation of the process parameters to achieve sound weld seams. Weld trials performed with the new tool still showed some tool wear in the weld seam, but the concentration was significantly lower. Figure 12 shows the microstructure of the weld center and the wear particle enriched zone on the advancing side.

To quantify the amount of wear on both tools, XRF-analyses by 10x10 mm spot on the advancing side of two weld seams have been performed (one with Mo and one with W-based tool). The results are given in Table 4. The increase in concentration for the weld seam performed with the Mo-based tool is 0,28 wt.% molybdenum versus 0,038 wt.% tungsten on the weld seam performed with the W-based tool compared to 0,01 wt.% molybdenum and 0,002wt% tungsten in the base metal.

To qualify the weld seam quality, additional mechanical tests have been performed. An example of an 5t bend (15mm S460 G2+M) test and a tensile test (10mm S460 G2+M), where the weld seam overmatched the base material according to DNVGL-ST-F101, are given in Figure 13 a) and b).[5]

Table 5 shows the micro hardness in the weld seam. The position of the measuring points was chosen according to DNVGL-ST-F101.[5]

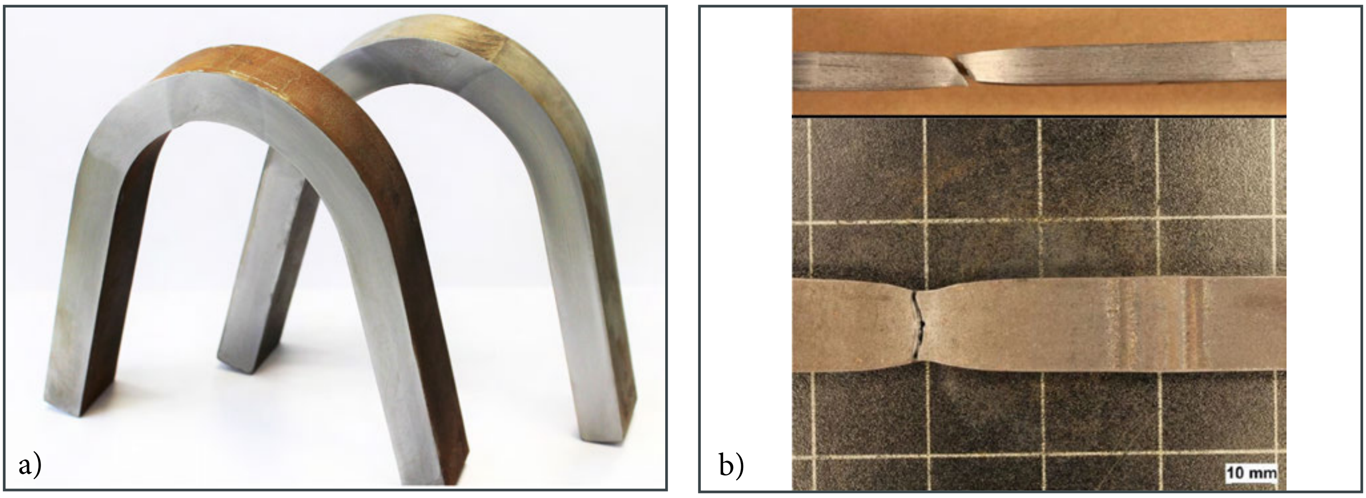

Figure 13: a) Root bend and face bend specimen of a 15mm S460 G2+M weld seam performed with a W-based tool and b) Tensile specimen from a 10mm S460 G2+M weld seam performed with a Mo-based tool

Table 5: Cross weld HV 10 hardness values for a 10mm S460 G2+M weld seam
Mean hardness values HV10

	Base metal AS	HAZ and TMAZ AS	Weld zone	HAZ and TMAZ AS	Base metal AS
cap	183	175	217	179	189
mid	177	177	206	177	179
root	177	172	204	175	180

Table 5: Cross weld HV10 hardness values for 10mm S460 G2+M weld seam Mean hardness values HV10

Figure 16: Cross section of a 14.3mm thick SMLS X65Q PSL2 pipe welded with a W- based tool

After achieving the required weld seam quality, the welding speed was increased up to 330 mm/min to decrease the weld cycle time and thus increase the cost saving potential. The welding speed was limited by the machine capacity.

4.5 S690 QL1 WELDING DEVELOPMENT

To show the potential of FSW on welding higher grade pipeline steel, the next step was to change to S690 steel grade. These changes in the base material led to some necessary changes in tool design, welding and preheating parameter. Comparing to the S460 weld trials, the higher steel grade tests were also performed on 10mm plates first and then the welding depth was increased to 15mm. After the W-based tool showed less wear and a higher stiffness in the previous work, the same material was used for this welding development. Compared to the 15mm thick S460 weld trials, the downforce was increased by 18% and the resulting spindle torque by 15% when welding 15 mm thick S690 steel grade. First visual inspection of the cross section of a 15mm thick weld seam indicated a higher tool wear on the higher steel grade. XRF analysis, shown in Table 6, confirmed this assumption. The amount of tungsten was 8.4 times higher on 15mm thick S690 compared to S460. After achieving flawless weld seams quality tests were started by checking the hardness values in the weld seam. The hardness profile, illustrated in Figure 14b shows a drop in the HAZ and thermomechanical affected zone and a slight increase in the weld zone (but still lower than the base metal).

Table 6: Tungsten wear in weld seams produced with W-based tools
XRF-analysis [wt.-%], advancing side

Element	Base metal S690 QL	Base metal S460 G2+M	15mm thick S690 QL welded with W-based tool	15mm thick S460 G2+M welded with W-based tool
W	0,002	0,002	0,126	0,015

Table 6: Tungsten wear in weld seams produced with W-based tools XRF-analysis [wt.-%], advancing side

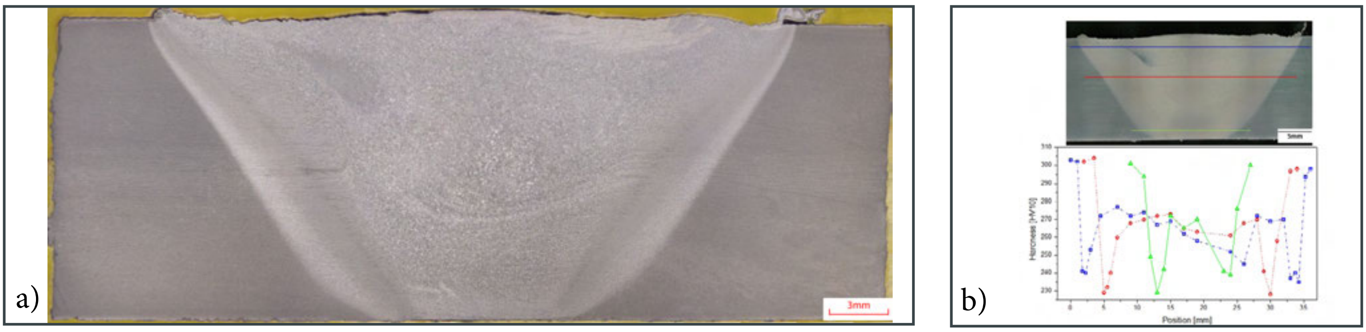

Figure 14 : a) Cross section of a 15mm S690 QL weld seam performed with a W- based tool and b) the related hardness values

4.6 PIPE WELDING ADAPTATION

The adaptation of the welding parameters developed on plate to circumferential pipe welding required 1) the development of the suitable welding equipment and backing system and 2) a sensitivity analysis on the transferability of the welding and preheating parameters from a flat to a curved surface.

In the initial stage of the pipe welding adaptation, it has been decided to opt for the AWS 1G welding position where the pipe is in the horizontal position and is rotated along its axis. The welding tool remains stationary as to its X and Y axis. During plunging and retraction, the tool can move along its Z axis. It can be noted that, although it is understood that a production-ready FSW pipe welding machine would have to be an orbital machine on a fixed pipe (AWS 5G/6G configurations), it is more convenient to use the 1G position during development work. The FSW process being virtually insensitive to gravity, a transfer between 1G to 5G/6G position is not anticipated as being an issue. The design of a backing system on pipe is more complex than on plate and required the design of an internal clamping device able to expand radially inside the pipe to provide a local support under the weld zone.

Table 7: Chemical composition of the pipe material (wt. - %)

Steel grade	C	Si	Mn	P	Cr	Ni	Cu	Mo	Ti
SMLS X65Q PSL 2	0,099	0,240	1,320	0,015	0,077	0,148	0,178	0,135	0,002

Table 7: Chemical composition of the pipe material (wt.-%)

The selected pipe material was an API 5L seamless X65Q PSL 2 of dimensions 323.8mm OD x 14.3mm WT. The pipe chemical composition is detailed in Table 7.
The reference welding parameters were based on the welding procedure established on plate 15mm S460 G2+M.

4.6.1 INITIAL TRIALS AT 10MM WITH MO-BASED TOOL

First trials were performed with the 10 mm Mo-based tool to check the comparability of plate and pipe welding behavior. The results showed a higher necessary welding force (downforce) to achieve the same results as on plates. This may be linked to the changes in thermal mass of the test setup (1400mm long pipes compared to 300mm wide plates) or the slight differences in the used materials (S460 G2+M plates compared to SMLS X65Q PSL2 pipes). After an increase of the downforce by 9%, good results were achieved. Figure 15 shows the resulting weld seam on a pipe.

4.6.2 14.3MM THICK SMLS X65Q PSL2 PIPE WELD TRIALS

With the knowledge of the different welding behavior between the weld trials on plates and on pipes from the 10mm Mo tool test, the full 14,3mm wall thickness was welded. Again, the tungsten-based tool was used for the higher welding depth.

Figure 15: Weld bead on SMLS X65Q PSL2 pipe done with 10mm Mo-based tool

Figure 16 shows a cross section of a 14.3mm thick SMLS X65Q PSL2 pipe welded with a tungsten-based tool. This part of the project is still ongoing and aims to reach the necessary weld seam quality according to DNVGL-ST-F101.

4.7 DISCUSSION

Less tool wear and higher hardness values and strength in the weld nugget may probably be achieved by decreasing the overall heat input during welding and preheating. However, this results in higher process loads and especially in a higher spindle torque that was initially limited by the machine's capacity. Sound friction stir welds on the 15mm thick S690 material could only be produced by utilizing an increased heat input by preheating at relatively low welding speeds. Higher welding speeds result in a higher radial and axial forces as well as spindle torques. In the present study, Mo-based FSW-tools seem to be unsuitable for joining of thick steels due to their susceptibility to deformation and abrasive wear. W-based tools seem more promising for such applications due to their improved hardness, strength and toughness at elevated temperatures. Nevertheless, certain tool wear could still be observed with both tools. The localized tungsten-rich zone on the advancing side of the weld can likely be prevented by using features such as threads on the probe. It is well known that, in such case, most of the wear occurs at the threads and is accelerated once features are used.6 This may markedly influence the stirring property and lifetime of the tool. If a tougher tool material (higher wear resistance) could be found, the use of features on the probe could be a promising option to improve the stirring. The process adaptation to pipe welding was possible thanks to the machine upgrade and the pipe rotator system and internal backing clamp. Further work is needed to develop the end hold extraction procedure on a curved surface.

5 CONCLUSIONS

The development program showed that friction stir welding for steel pipeline fabrication is a promising technology. Sound weld seams according the DNVGL standard were produced.5 One major point for optimization is the reduction of the tool wear. As shown in the paper, choosing the right tool material and the use of a preheating process can reduce it significantly. The preheating also affects the welding parameter and reduces the needed loads on the machine. The additional heat input from the preheating system reduces the amount of energy that must be generated by the tool. This has a direct effect on possible welding speed and machine design.

6 ACKNOWLEDGEMENTS

The author would like to acknowledge the contribution of the following organizations for their technical support, expertise and specialist testing for the development program:

- Graz University of Technology
- Vienna University of Technology

The authors would like to thank Subsea 7S for permission to publish this paper. However, its content only reflects the opinion of the authors and does not imply endorsement by the Company.

7 REFERENCES

1. G. Sorger, E. Lehtimäki, S. Hurme, H. Remes, P. Vilaça, L. Molter, "Microstructure and fatigue properties of friction stir welded high-strength steel plates", Science and Technology of Welding and Joining, (UK, Taylor & Francis Group, 2017).
2. A. Kumar, D. Fairchild, M. Macia, T. Anderson, "Evaluation of economic incentives and weld properties for welding steel pipelines using friction stir welding", 21st International Offshore and Polar Engineering Conference (Maui, Hawaii, USA, June 19-24, 2011).
3. B. M. Tweedy, W. Arbegast, and C. Allen, Friction Stir Welding and Processing, 3rd ed. (Cham, Switzerland: Springer, 2005) p. 97–104.
4. A. I. Alvarez, V. Cid, G. Pena, J. Sotelo, and D. Verdera, Friction Stir Welding and Processing, 7th ed. (Cham, Switzerland: Springer, 2016), p. 117–126.
5. DNVGL-ST-F101 2007, "Submarine pipeline systems"
6. J. Peterson, J. G. Perrett, R. Steel, and Q. Liu, "Evaluation of Advanced Tool Material Technology for the Friction Stir Welding of 6mm AISI 304L Stainless Steel and 6mm A36 Cold Rolled Mild Steel," in 8th International Symposium on Friction Stir Welding, 2010, Timmendorfer Strand, Germany, pp. 962–972.
7. G. Toguyeni, O. Caliskanoglu, C. Pfeiffer, "Reduction of Tool Wear and Loads During Friction Stir Welding of Steel for Pipeline Fabrication", Materials Performances & Welding Technologies 2019, paper no. MPWT19-14275 (Dammam, Saudi Arabia, NACE 2019).

Authors

Grégory Toguyeni

Subsea 7 France

Principal Welding and Materials Engineer

gregory.toguyeni@subsea7.com

Christian Pfeiffer

Stirtec GmbH

R&D Engineer

christian.pfeiffer@stirtec.at

Dr Ozan Caliskanoglu

Stirtec GmbH

R&D Engineer

ozan.caliskanoglu@stirtec.at

Lucas Oppeneiger

Stirtec GmbH

R&D Engineer

lucas.oppeneiger@stirtec.at